The cell and stress specific dynamics of *in vivo* and *in vitro* canonical and non-canonical tRNA cleavage.

Sherif Rashad, MD, PhD[1,2]*. Takaaki Abe, MD, PhD[3-5]. Teiji Tominaga, MD, PhD[2]. Kuniyasu Niizuma, MD, PhD[1,2,6].

1- Department of Neurosurgical Engineering and Translational Neuroscience, Tohoku University Graduate School of Medicine, Sendai, Japan.
2- Department of Neurosurgery, Tohoku university Graduate School of Medicine, Sendai, Japan.
3- Division of Nephrology, Endocrinology, and Vascular Medicine, Tohoku University Graduate School of Medicine, Sendai, Japan
4- Department of Clinical Biology and Hormonal Regulation, Tohoku University Graduate School of Medicine, Sendai, Japan
5- Department of Medical Science, Tohoku University Graduate School of Biomedical Engineering, Sendai, Japan
6- Department of Neurosurgical Engineering and Translational Neuroscience, Graduate School of Biomedical Engineering, Tohoku University, Sendai, Japan.

***Corresponding author details:**

Sherif Rashad, M.D., Ph.D.

2-1 Seiryo-machi, Aoba-ku, Sendai 980-8575, Japan
Phone: +81-22-717-7230
Fax: +81-22-717-7233
E-mail: sherif@nsg.med.tohoku.ac.jp , sherif_rashad@hotmail.com

Abstract:

Following stress, tRNA is cleaved to generate tRNA halves (tiRNAs). These stress induced small RNAs have been shown to regulate processes such as translation initiation and stem cell function. To date, angiogenin (ANG) is considered the main enzyme that cleaves tRNA at its anti-codon site to generate 35 ~ 45 nucleotide long 5' and 3' tiRNA halves. Herein, using rat model of focal ischemia and 2 different rat neuronal cell lines exposed to different stresses, we show that tRNA cleavage is a selective process that is heterogenous amongst different tRNAs. We also report for the first time the existence of non-canonical tRNA cleavage that is angiogenin independent and that tRNA cleavage is cell specific and stress specific. Moreover, we show that angiogenin-mediated tRNA cleavage itself is tRNA selective and that angiogenin overexpression doesn't lead to the expected overt tRNA cleavage in the cells. Finally, the proposed enzymes responsible for this non-canonical tRNA cleavage do not appear to be regulated by RNH1, the angiogenin inhibitor.

Keywords: Biomarkers; Cerebral ischemia; Epigenetics; non-coding RNA; Small RNA; Stroke; tiRNA; tRNA; tRNA cleavage.

Introduction

tiRNAs are small non-coding tRNA derived fragments that are produced via tRNA cleavage during stress and are also present under physiologic conditions (Goncalves et al., 2016; Rashad et al., 2020b). tRNA cleavage's regulation and exact functions are still not fully understood. While Angiogenin (Ang) is identified as the main enzyme responsible for the generation of tiRNA fragments (Elkordy et al., 2018; Yamasaki et al., 2009), there are studies hinting to other enzymes being involved in this process that are yet to be identified (Krishna et al., 2019). Moreover, does these small RNAs play a role beyond the reported protein translation repression or not is still not known (Emara et al., 2010; Ivanov et al., 2011; Ivanov et al., 2014; Rashad et al., 2020b). There are also contradictory results in the literature regarding their protective or cytotoxic effects in the cells (Ivanov et al., 2014; Thomas et al., 2018). Our previous results hints to a cytotoxic effect of tiRNAs, as neuroprotective therapy reduced tRNA cleavage (Elkordy et al., 2019), similar to other reports indicating a cytotoxic effect of tiRNAs (Thomas et al., 2018). However, other groups have reported protective effects of tiRNAs via protein translation repression, stress granule assembly and cytochrome *c* quenching (Ivanov et al., 2011; Ivanov et al., 2014; Saikia et al., 2014). Thus, more studies are needed to address these differences and identify their root causes, whether they are cell or tissue specific or cell stress pathway specific.

The cleavage process of tRNA was shown to be regulated, at least at some level, via tRNA methylation modifications such as 1-methyadenosine (m^1A) modifications and 5-methylcytosine (m^5C) modifications via a variety of tRNA methyltransferases or demethylases (Chen et al., 2019; Kawarada et al., 2017; Liu et al., 2016; Rashad et al., 2020a; Tuorto et al., 2012). This indicates a higher-level regulation rather than a global cleavage pattern, since not all tRNA species are equally modified and the affinity of certain tRNA methylation modifying enzymes is selective to particular tRNAs (Chen et al., 2019; Kawarada et al., 2017; Liu et al., 2016).

Here we wanted to explore this proposed specificity of tRNA cleavage following *in vivo* and *in vitro* stresses and using different cell lines and different stressors. We discovered that not all tRNAs are cleaved equally, and that the cleavage sites are varying between different tRNAs and also between different cell lines. We here report a non-canonical pattern of tRNA cleavage that is yet to be explored in the terms of its effectors. We also explored the

specificity of angiogenin to tRNA cleavage and whether angiogenin is responsible for this so called non-canonical tRNA cleavage.

Results and Discussion

tRNA is cleaved after tMCAO in a tRNA-species specific manner

tMCAO was previously shown to induce tRNA cleavage (Li et al., 2016). We observed that the maximum tRNA cleavage is observable 24 hours after reperfusion (Data not shown). Thus, we selected this time point for our evaluation.

Next, we wanted to evaluate if tRNA cleavage after I/R injury is a global phenomenon or specific to particular tRNA-species. We used DIG-labeled probes to evaluate individual cytosolic and mitochondrial tRNA species cleavage 24 hours after reperfusion (Figure 1).

Following I/R, the cleavage pattern was selective to particular species. tRNA-Arg^{CCT} , was not cleaved *in vivo*. Also, tRNA-Met^{CAT} (also known as initiator tRNA-Met or tRNA^{iMET}) was not cleaved after I/R. While tRNA-Gly^{GCC}, tRNA-Leu^{AAG} and tRNA-Ala^{AGC} were robustly cleaved. tRNA-Gln^{CTG} was only minimally cleaved, and the membrane needed extended exposure periods in order to reveal the 5'tiRNA fragments resulting from this cleavage.

Mitochondrial tRNAs were also cleaved, as evident from the analysis of several mt-tRNAs. Interestingly, the phenotypical appearance of the cleavage pattern appears to deviate from the canonical angiogenin-mediated tRNA cleavage visible with cytosolic tRNA species in some of the mitochondrial tRNA species. While the 5'tiRNA fragments resulting from cytosolic tRNA cleavage were typically between the 35 to 45 nucleotide mark, indicating canonical cleavage at the anti-codon, the 5'tiRNA fragment from mt-Tyr^{GTA} , mt-Ala^{TGC} and some mt-Asn^{GTT} fragments were much larger, being detected between 50 and 60 nucleotides mark. mt-Asn^{GTT} GTT cleavage was bimodal, with fragments at the canonical size of 35 to 45 nucleotides and other non-canonical larger fragments similar to what was observed with mt-Tyr^{GTA} . mt-Met^{CAT} and mt-Gly^{TCC} were largely canonically cleaved, although mt-Met^{CAT} exhibited several larger non-canonical 5' fragments as well.

These findings indicate that the process of *in vivo* cleavage of tRNA is vastly different between cytosolic and mitochondrial tRNAs, at least for the tested tRNAs. It also clearly indicates the presence of other cleavage sites (other than the anti-codon) for the generation of stress induced tiRNAs.

In vitro tRNA cleavage is cell line and stress specific and shows non-canonical fragments

In this step, we wanted to evaluate the cleavage pattern of tRNA *in vitro*. In particular, we wanted to evaluate whether tRNA can be cleaved non-canonically *in vitro* and whether the cleavage patterns are the same under different stress conditions and in different cell lines. We exposed PC12 and B35 cells (both rat neuronal cell lines) to oxidative stressors using toxic doses of sodium meta-Arsenite (As) (Elkordy et al., 2018) and Antimycin A (AM), which targets mitochondrial respiratory complex III (Zhou et al., 2011). Exposure of PC12 cells to As led to induction of apoptosis and robust tRNA cleavage (Supplementary figure 1A), while exposure to 200µg/ml of antimycin A, a dose that is 20 times the reported to induce pyroptosis and inflammasome activation in other cell lines (Zhou et al., 2011), did not have significant effect on cell viability or gross tRNA cleavage. On the other hand, both As and antimycin A induced cell death and tRNA cleavage in B35 cells as evident by Annexin V assay and SYBR gold staining (Supplementary figure 1B). This indicates that observable tRNA cleavage is synonymous with initiation of cell death, and that cellular responses to different stressor dictates tRNA sensitivity to cleavage and gross tiRNA generation.

To examine this notion, we used DIG-labeled DNA probes to evaluate individual tRNAs' cleavage in both cell lines following As and antimycin stresses. First, we examined cytosolic tRNA cleavage in PC12 and B35 cells after As or antimycin stresses (Figure 2). We observed several differences in the cleavage patterns of tRNA between PC12 and B35 cells.

Leu^{AAG} showed quite an interesting pattern of cleavage under different stresses and between the 2 cell lines. While As stress caused canonical cleavage of Leu^{AAG} in both cell lines, antimycin stress caused an enrichment of a non-canonical 5'half in PC12 cells with minimal enrichment of the canonical 5'halves. On the contrary, antimycin stress led to canonical cleavage of Leu^{AAG} in B35. Considering that PC12 cells were resistant to antimycin stress, there is an apparent correlation between the non-canonical cleavage of Leu^{AAG} and cellular responses to ischemia. Such a correlation needs further analysis, indeed, to evaluate if there is a causative link between this process and cellular fate. Therefore, efforts to sequence the nan-canonical fragments of Leu^{AAG} as well as other tRNAs should be sought after.

Ala^{AGC} was only cleaved after As stress in PC12 canonically, but not after AM stress. It was cleaved both canonically and non-canonically after AM stress in B35 with minimal cleavage after As stress in B35 cells.

Gly^{GCC} was cleaved canonically in both cell lines, although antimycin stress in PC12 cells did not lead to its cleavage. Gln^{CTG} was only cleaved in B35 cells into a canonical 5'tiRNA

fragment after both stresses and an extra non-canonical fragment only after antimycin stress. Met^{CAT} was not cleaved in both cell lines. Arg^{CCT} was cleaved non-canonically after antimycin stress in B35 cells only resulting in a large 5'tiRNA fragment. Lys^{CTT} was cleaved into 2 5'tiRNA fragments after As stress in PC12 and after As and antimycin stresses in B35. Both fragments were within the canonical range of tiRNAs (i.e 35 ~ 45 nt) suggesting that the cleavage occurred at the anticodon and at a nearby site. Moreover, Lys^{CTT} showed a large non-canonical tiRNA fragment after antimycin stress in B35 cells. Glu^{CTC} was also cleaved canonically after As stress in PC12 and after As and antimycin stresses in B35 with a non-canonical tiRNA fragment observed after both stresses in B35, albeit more evident after antimycin stress.

Mitochondrial tRNA cleavage also showed observable differences between PC12 and B35 cell lines (Figure 3). mt-Tyr^{GTA} was cleaved after As stress in PC12 (in a more or less degradation-like manner with many fragments observable) while it was cleaved canonically and non-canonically after antimycin stress in B35 but not As stress. mt-Met^{CAT} showed non-canonical cleavage after As and antimycin stresses in PC12 cells, although to a higher degree with As stress, while no observable cleavage was noted in B35 cells. mt-Asn^{GTT}, mt-Gly^{TCC}, mt-Ala^{TGC} and mt-Arg^{TCG} were not cleaved in both cell lines.

It's notable to observe the differences exist not only between these cell lines under the same stress, but also between *in vivo* and *in vitro* patterns of tRNA cleavage and the species cleaved. Collectively, these results indicate a stress, cell type and tRNA specific pattern of cleavage rather than a global non-specific cleavage mechanism. These results also show that non-canonical cleavage is specific and not a result of haphazard degradation of tRNA, since the same tRNA species were non-canonically cleaved in certain conditions and not the others.

Overall, we observed non-canonical cleavage *in vivo* to occur in mitochondrial tRNAs and *in vitro* to be more evident with the mitochondrial targeting stressor antimycin. This suggests a big role played in mitochondrial stress and dynamics in regulating canonical versus non-canonical tRNA cleavage.

Ang and RNH1 overexpression; impact on tRNA cleavage after stress

Angiogenin is currently regarded as the main enzyme involved in tRNA cleavage (Emara et al., 2010; Ivanov et al., 2011; Ivanov et al., 2014; Lyons et al., 2017; Yamasaki et al., 2009). RNH1 is the angiogenin inhibitor (Furia et al., 2011; Pizzo et al., 2013; Saikia et al., 2012;

Thomas et al., 2018; Yamasaki et al., 2009), and its knockout was reported to increase cytotoxicity via what believed to be Angiogenin induced tRNA cleavage (Thomas et al., 2018). Here we sought to answer two questions. First, is Angiogenin responsible for the non-canonical tRNA cleavage we observed? And if not, what is the enzyme or possible enzymes responsible for this process? The second question was; how specific is the Angiogenin mediated tRNA cleavage, and does Angiogenin cleave all tRNAs?

To answer these questions, we introduced DNA plasmids to overexpress human Angiogenin (hAng), as we reported previously (Elkordy et al., 2018), or RNH1 into PC12 cells (Figure 4A and B). Then we exposed the cells to As (400µM) or antimycin (200µg/ml) stresses for 4 hours and observed the impact of hAng or RNH1 overexpression on gross tRNA cleavage as well as species-specific tRNA cleavage.

First, hAng overexpression in PC12 cells increased gross tRNA cleavage following As stress and not antimycin stress as observed by SYBR gold staining (Figure 4C). RNH1 overexpression, however, did not lead to the expected effect of suppressing tRNA cleavage (Figure 4D).

To further characterize these findings, we looked into several tRNA species' specific cleavage patterns following gene overexpression (Figure 5). Leu^{AAG}, which showed canonical and non-canonical 5'tiRNA fragments especially after antimycin stress, showed an interesting pattern. While hAng enhanced the canonical Leu^{AAG} 5'tiRNA fragments especially after antimycin stress, it had no effect on the larger non-canonical fragments. Moreover, RNH1 overexpression reduced the canonical 5'tiRNA fragments following antimycin stress and not after As stress, and again had no impact on the non-canonical fragments.

Lys^{CCT}, Ala^{AGC} and Gly^{GCC} expressed a modest increase in cleavage following hAng overexpression, while RNH1 suppressed their cleavage. Notably, these tRNAs showed little changes with RNH1 expression following As stress.

Glu^{CTG} did not exhibit significant changes in the levels of its 5'tiRNA fragments after hAng or RNH1. mt-Met^{CAT}, which is cleaved mainly non-canonically, showed an opposing effect. It appears that hAng overexpression reduced the non-canonical cleavage, while inhibiting angiogenin via RNH1 overexpression mildly enhanced this cleavage pattern.

These results indicate that the impact of angiogenin on tRNA cleavage is not only stress specific, but it is also limited to specific tRNA species, and it is not as extensive as previously thought (a finding that was recently corroborated by other researchers (Su et al., 2019)). Moreover, it indicates that angiogenin has no impact on the non-canonical 5'tiRNA fragments generation. We hypothesize that it rather may be competing with another unknown enzyme for the cleavage sites of tRNA, as evident in mt-Met^{CAT}. Thus, when angiogenin has higher affinity to a given tRNA, canonical cleavage takes the upper hand, and vice versa. Unfortunately, sequencing efforts from knockout cell lines did not account for such a hypothesis as the non-canonical cleavage and existence of large tiRNAs was not reported previously to the best of our knowledge. Therefore, such non-canonical fragments were probably excluded from the analysis of the sequencing data as they are larger than the usually focused on canonical fragments .

Summary and conclusion:

We report for the first time the existence of stress induced non-canonical tRNA cleavage that does not involve angiogenin and that occurs at regions not involving the anti-codon segment of tRNA, as apparent from the 5'tiRNA fragment size. This should be taken in consideration in future works involving the use of next generation sequencing technology, as these larger fragments were not previously reported probably due to the filtration processes that would inadvertently exclude these larger fragments from downstream analysis. Sequencing different tiRNAs with different cleavage sites and sizes can lead to further understanding of the functional differences between canonical and non-canonical tRNA cleavage and what different tiRNAs can bind to or regulate. Moreover, we show that the process of canonical cleavage itself must include enzymes other than angiogenin. This stems from the fact that RNH1 overexpression failed to reduce the gross tRNA cleavage and also failed to impact several tRNAs studied here and that angiogenin overexpression did not increase the cleavage of all tRNAs studied and when it did, it was not uniform under different stresses. Previously, only RNH1 knockdown or knockout were attempted in the context of stress induced tRNA cleavage (Thomas et al., 2018; Yamasaki et al., 2009). This would in essence leave angiogenin, as well as other RNases unchecked leading to enhanced tRNA cleavage. However, the failure of RNH1 to impact non-canonical tRNA cleavage or the cleavage of several tRNA species indicates that the other proposed tRNA cleaving enzymes do not belong in the group of enzymes inhibited by RNH1. Finally, angiogenin showed an apparent selectivity to the tRNAs it enhanced its cleavage after overexpression. This indicates a higher

level of functional regulation that is yet to be explored. This regulation could be on the level of tRNA modifications (Rashad et al., 2020b) or at the protein level (i.e. several enzymes competing for tRNA cleavage for example as we hypothesized). Recently, we reported the impact of the tRNA m^1A demethylase Alkbh1 on regulating tRNA cleavage (Rashad et al., 2020a). Based on our findings, m^1A demethylation via Alkbh1 impacted tRNA cleavage in a stress specific manner *in vitro*. Moreover, we observed differences between canonical and no-canonical fragments' expression after Alkbh1 overexpression or knockdown, indicating the contribution of tRNA methylation to the regulation of canonical versus non-canonical tRNA cleavage. Interestingly, the impact of Alkbh1-induced demethylation on tRNA cleavage was significantly more robust than overexpressing human angiogenin (Rashad et al., 2020a). While we acknowledge there is a lot to be explored in terms of the presented work, we hope our work will stimulate further research into this interesting non-canonical process of stress induced tRNA cleavage.

Methods

Animals: transient middle cerebral artery occlusion (tMCAO) was induced in 8 weeks old, 180-200gm male Wistar rats as previously described (Faheem et al., 2019). Animals were bought from a local vendor (Kumagai-Shoten Sendai) and housed in a controlled environment with 12 hours light/dark cycle and temperature regulated at 23°C. Animals were allowed to acclimatize for at least 24 hours before any experimental procedures. All experiments were conducted according to protocols approved by the animal care facility of Tohoku University (Ethical approval number 2017MdA-137-3) and according to the ARRIVE (Animal Research: Reporting In Vivo Experiments) guidelines. All animal surgeries were performed between 9am and 4pm. No blinding was performed for this work.

Animal model for transient middle cerebral artery occlusion (tMCAO): The ischemia-reperfusion model was performed as described previously (Faheem et al., 2019). In brief, after induction of anesthesia using inhalation anesthesia by 66% nitrous oxide and 33% oxygen plus 1.5% isoflurane gas mixture, a midline incision was performed, carotid bifurcation exposed, external carotid artery ligated and incised and a coated occlusion suture (4035PKRe5, Doccol, Corp., Sharon, MA, http://www.doccol.com/) was inserted to occlude the middle cerebral artery for 60 min. After the occlusion period the suture was removed to induce reperfusion injury, the wound sutured, and the animals allowed to rest before being sacrifice at the designated time points based on a simple randomization scheme designed in Excel (Microsoft corp.). after reperfusion. Animals from were sacrificed after 24 hours. Sham animals were prepared by performing all the surgical steps without suture occlusion of the MCA.

Cell culture and *in vitro* stress: 2 cell lines were used in this study. PC12 (rat pheochromocytoma cell line, ATCC, Cat# CRL-1721) and B35 (rat neuroblastoma cell line, ATCC, Cat# CRL-2754). PC12 was cultured in RPMI 1640 medium (Wako, Osaka, Japan. Cat# 189-02025) supplemented with 10% heat inactivated horse serum (Gibco, Japan. Cat# 16050-122) and 5% fetal bovine serum (FBS, Hyclone, GE-life sciences, USA. Cat# SH30910.03). B35 cells were cultured in high glucose DMEM medium (Nacalai Tesque, Cat# 08457-55) supplemented with 10% FBS. Cellular stress was performed by adding sodium meta-Arsenite (Sigma-Aldrich, Cat# S7400-100G) or streptococcal antimycin A (Sigma-Aldrich, Cat# A8674) at the designated concentrations and durations to the cells in full growth medium.

Plasmid transfection: 1×10^6 cells (PC12 cell line) were cultured per well in a 6 well plate coated by Poly-L-Lysine. FLAG-tagged human angiogenin plasmid (Cat # RC208874; OriGene; Rockville, MD), GFP-tagged rat RNH1 plasmid (Cat# ORa42809C, Genescript; Tokyo, Japan) or Mock plasmid were transfected to the cells using Lipofectamine 3000 (Thermo Fischer, Cat# L3000015) as per manufacturer's protocol in full growth medium without antibiotics. Three days after transfection the cells were evaluated for transfection efficiency using western blotting. Cell stress was performed 72 hours after transfection as per experimental protocol.

RNA isolation and extraction: At the designated time-points animals were euthanized using overdose isoflurane anesthesia and then transcardiac perfusion using ice cold saline was performed. Brains were extracted and sliced on a matrix and the middle third of the left cerebral hemisphere was lysed in Qiazol (Qiagen, Hilden, Germany, Catalog# 79306). RNA was extracted using the miRNeasy micro kit (Qiagen, Hilden, Germany, Catalog# 217084) with a DNase digestion step as per manufacturer's protocol. RNA concentration was analyzed using nanodrop one (Thermo Fisher Scientific, San Jose, CA, Catalog# ND-ONE-W).

Northern blot and SYBR gold staining: tiRNA generation using SYBR gold staining was performed as we previously described(Elkordy et al., 2018; Elkordy et al., 2019). In brief, 4µg of total RNA were loaded per well after denaturation by heating at 70°C for 3 minutes in sample buffer (Novex TBE-Urea sample buffer; Thermo fisher Scientific, Catalog# LC6876). Samples were electrophoresed using Novex 15% TBE-Urea Gels (Invitrogen, Carlsbad, CA, Catalog# EC68755;) in 1x TBE buffer (Bio-Rad, Catalog# 161-0733). Gels were then incubated with 10,000-fold diluted SYBR Gold nucleic acid gel stain (Life technologies, Eugene, OR, Catalog# S11494) in 0.5× TBE buffer for 30 min at room temperature. Stained gels were visualized using Chemi-Doc MP Imager (Bio-Rad, Hercules, CA) and analyzed by Image Lab Software (Bio-Rad, Hercules, CA. RRID# SCR_014210).

DIG-labeled probes based tiRNA detection:

Detection of individual tRNA and tRNA species using targeted DIG-labeled probes was performed as we reported previously(Elkordy et al., 2018; Elkordy et al., 2019). Following membrane transfer and cross linking, membranes were pre-hybridized in DIG Easy Hyb solution (Roche, Catalog# 11603558001) for 30 minutes at 40°C followed by overnight incubation at 40°C with 1 µg/ml DIG-labeled DNA probes in DIG Easy Hyb solution with

continuous agitation. After two low stringency washes for 5 minutes each with 2× saline sodium citrate/ 0.1% sodium dodecyl sulfate buffer (2x SSC buffer; Promega Co., Madison, WI, Catalog# V4261) and a high stringency wash for 2 min with 1x SSC buffer, the membrane was blocked in blocking reagent (Roche, Catalog# 11585762001) for 30 min. The membranes were then probed with alkaline phosphatase labeled anti-DIG antibody (Roche, Catalog# 11093274910) for 30 min, washed for 30 min with washing buffer (1 × maleic acid buffer + 0.3% Tween 20; Roche, Catalog# 11585762001), then equilibrated for 3 min in detection buffer (Roche, Catalog# 11585762001). Signals were visualized with CDP-Star Ready-to-Use (Roche, Catalog# 12041677001) and images taken with Chemi-Doc MP Imager.

Probe sequences used in this study were:

For cytosolic tRNA:

5'tRNA-Arg^{CCT}: 5'-AGGCCAGTGCCTTATCCATTAGGCCACTGGGGC

5'tRNA-Leu^{AAG}: 5'-AATCCAGCGCCTTAGACCGCTCGGCCATGCTACC

5'tRNA-Gln^{CTG}: 5'-AGTCCAGAGTGCTAACCATTACACCATGGAACC

5'tRNA-Gly^{GCC}: 5’-GCAGGCGAGAATTCTACCACTGAACCACCAATGC

5'tRNA-Ala^{AGC}: 5’-CTAAGCACGCGCTCTACCACTGAGCTACACCCCC

5’tRNA-Met^{CAT}: 5’GACTGACGCGCTACCTACTGCGCTAACGAGGC

5’tRNA-Lys^{CTT}: 5’GTCTCATGCTCTACCGACTGAGCTAGCCGGGC

5’tRNA-Glu^{CTC}: 5’GCGCCGAATCCTAACCACTAGACCACCAGGGA

For mitochondrial tRNA:

5'mit-tRNA-Asn^{GTT}: 5'-AGCTAAATACCCTACTTACTGGCTTCAATCTA

5'mit-tRNA-Tyr^{GTA}: 5'-AGTCTAATGCTTACTCAGCCACCCCACC

5’mt-tRNA-Met^{CAT}: 5’CCCGATAGCTTAGTTAGCTGACCTTACT

5’mt-tRNA-Arg^{TCG}: 5’TCATTAATTTTATTTAAACTAATTACCA

5’mt-tRNA-Gly^{TCC}: 5’GTCAGTTGTATTGTTTATACTAAGGGAGT

5’mt-tRNA-Ala^{TGC}: 5’ATCAACTGCTTTAATTAAGCTAAATCCTC

Sequences for Cytosolic tRNAs were acquired from GtRNAdb (http://gtrnadb.ucsc.edu/) and for mitochondrial tRNAs from mitotRNAdb (http://mttrna.bioinf.uni-leipzig.de/mtDataOutput/).

Following acquisition of images using the DIG-labeled probes, membranes were stripped using 0.1x SSC – 0.5% sodium dodecylsulphate (SDS) solution at 80ºC for 30 minutes then washed briefly in PBS-T and re-probed or stored in 5x SSC buffer for long term storage at 4ºC.

Western blotting:

Following plasmid transfection, cells were collected and lysed in NE-PER nuclear and cytoplasmic extraction reagent (Thermo Fischer, Cat# 78833). The protein content was determined using the Brachidonic-acid assay kit (Thermo Fisher Scientific, Cat# 23227). Equal loads of proteins were separated with the Mini-PROTEAN TGX system (Bio-Rad Laboratories) and transferred to polyvinylidene difluoride membrane (Bio-Rad Laboratories). Membranes were incubated with antibody against RNH1 (1:500, Sigma Aldrich, Cat# SAB2103138) or with anti-FLAG antibody (1:400, Sigma Aldrich, Cat# F3165) overnight at 4□. After incubation with horseradish peroxidase-conjugated secondary antibody (IgG detector, Takara Clontech, Cat# T7122A-1), the antigen was detected using chemiluminescence Western blotting detection reagents (Pierce ECL Western Blotting Substrate, Thermo Fisher Scientific Inc., Rockford, IL, the USA, Cat# 32106). The image was scanned with ChemiDoc (Bio-Rad Laboratories). Membranes were striped using stripping buffer (Restore Western Blotting Stripping Buffer, Thermo Fisher Scientific Inc., Cat# 21059) and re-probed using anti-beta actin (1:5000, Rabbit IgG, Cell Signaling Technology, Cat# 13E5) using the same steps that were used previously. Semi-quantification was performed utilizing the ImageJ software after correcting the signal to an internal control (beta-actin).

Annexin V flowcytometry (FACS) assay

Apoptosis and cell death were analyzed using flowcytometry Annexin V assay as per our published protocol (Elkordy et al., 2019). In brief, following exposure to stress in 24 well plate, cells were collected by trypsinization using 0.25% Trypsin in EDTA and washed using Annexin V binding buffer (0.5% bovine serum albumin (BSA) + 0.2mM Calcium Chloride in

Fluorobrite DMEM medium [Gibco, Cat# A18967-01]). Then, cells were incubated with Alexa Fluor 647 Annexin V antibody (Biolegend, Cat# 640943) and Propidium Idodie (Invitrogen, Cat# P3566) for 15 minutes. The samples were analyzed using FACS canto II.

Acknowledgment: The authors report no conflict of interest nor there are any ethical adherences regarding this work.

Funding: This work was partially supported by JSPS KAKENHI Grant Numbers 17H01583. The authors report no conflict of interest regarding this work.

Author contribution: Rashad: Conception and study design, administration, conducted all experiments, analyzed the data and wrote the manuscript. **Niizuma:** Funding acquisition and administration. **Niizuma, Abe, Tominaga:** critically revised the manuscript. **All authors:** approved the final version of the manuscript.

References:

Chen, Z., M. Qi, B. Shen, G. Luo, Y. Wu, J. Li, Z. Lu, Z. Zheng, Q. Dai, and H. Wang. 2019. Transfer RNA demethylase ALKBH3 promotes cancer progression via induction of tRNA-derived small RNAs. *Nucleic acids research*. 47:2533-2545.

Elkordy, A., E. Mishima, K. Niizuma, Y. Akiyama, M. Fujimura, T. Tominaga, and T. Abe. 2018. Stress-induced tRNA cleavage and tiRNA generation in rat neuronal PC12 cells. *J Neurochem*. 146:560-569.

Elkordy, A., S. Rashad, H. Shehabeldeen, E. Mishima, K. Niizuma, T. Abe, and T. Tominaga. 2019. tiRNAs as a novel biomarker for cell damage assessment in in vitro ischemia-reperfusion model in rat neuronal PC12 cells. *Brain research*. 1714:8-17.

Emara, M.M., P. Ivanov, T. Hickman, N. Dawra, S. Tisdale, N. Kedersha, G.F. Hu, and P. Anderson. 2010. Angiogenin-induced tRNA-derived stress-induced RNAs promote stress-induced stress granule assembly. *J Biol Chem*. 285:10959-10968.

Faheem, H., A. Mansour, A. Elkordy, S. Rashad, M. Shebl, M. Madi, S. Elwy, K. Niizuma, and T. Tominaga. 2019. Neuroprotective effects of minocycline and progesterone on white matter injury after focal cerebral ischemia. *Journal of clinical neuroscience : official journal of the Neurosurgical Society of Australasia*. 64:206-213.

Furia, A., M. Moscato, G. Cali, E. Pizzo, E. Confalone, M.R. Amoroso, F. Esposito, L. Nitsch, and G. D'Alessio. 2011. The ribonuclease/angiogenin inhibitor is also present in mitochondria and nuclei. *FEBS letters*. 585:613-617.

Goncalves, K.A., L. Silberstein, S. Li, N. Severe, M.G. Hu, H. Yang, D.T. Scadden, and G.F. Hu. 2016. Angiogenin Promotes Hematopoietic Regeneration by Dichotomously Regulating Quiescence of Stem and Progenitor Cells. *Cell*. 166:894-906.

Ivanov, P., M.M. Emara, J. Villen, S.P. Gygi, and P. Anderson. 2011. Angiogenin-induced tRNA fragments inhibit translation initiation. *Molecular cell*. 43:613-623.

Ivanov, P., E. O'Day, M.M. Emara, G. Wagner, J. Lieberman, and P. Anderson. 2014. G-quadruplex structures contribute to the neuroprotective effects of angiogenin-induced tRNA fragments. *Proceedings of the National Academy of Sciences of the United States of America*. 111:18201-18206.

Kawarada, L., T. Suzuki, T. Ohira, S. Hirata, K. Miyauchi, and T. Suzuki. 2017. ALKBH1 is an RNA dioxygenase responsible for cytoplasmic and mitochondrial tRNA modifications. *Nucleic acids research*. 45:7401-7415.

Krishna, S., D.G. Yim, V. Lakshmanan, V. Tirumalai, J.L. Koh, J.E. Park, J.K. Cheong, J.L. Low, M.J. Lim, S.K. Sze, P. Shivaprasad, A. Gulyani, S. Raghavan, D. Palakodeti, and R. DasGupta. 2019. Dynamic expression of tRNA-derived small RNAs define cellular states. *EMBO Rep*.

Li, Q., B. Hu, G.W. Hu, C.Y. Chen, X. Niu, J. Liu, S.M. Zhou, C.Q. Zhang, Y. Wang, and Z.F. Deng. 2016. tRNA-Derived Small Non-Coding RNAs in Response to Ischemia Inhibit Angiogenesis. *Scientific reports*. 6:20850.

Liu, F., W. Clark, G. Luo, X. Wang, Y. Fu, J. Wei, X. Wang, Z. Hao, Q. Dai, G. Zheng, H. Ma, D. Han, M. Evans, A. Klungland, T. Pan, and C. He. 2016. ALKBH1-Mediated tRNA Demethylation Regulates Translation. *Cell*. 167:816-828 e816.

Lyons, S.M., M.M. Fay, Y. Akiyama, P.J. Anderson, and P. Ivanov. 2017. RNA biology of angiogenin: Current state and perspectives. *RNA biology*. 14:171-178.

Pizzo, E., C. Sarcinelli, J. Sheng, S. Fusco, F. Formiggini, P. Netti, W. Yu, G. D'Alessio, and G.F. Hu. 2013. Ribonuclease/angiogenin inhibitor 1 regulates stress-induced subcellular localization of angiogenin to control growth and survival. *Journal of cell science*. 126:4308-4319.

Rashad, S., X. Han, K. Sato, E. Mishima, T. Abe, T. Tominaga, and K. Niizuma. 2020a. The stress specific impact of ALKBH1 on tRNA cleavage and tiRNA generation. *bioRxiv*:2020.2001.2031.928234.

Rashad, S., K. Niizuma, and T. Tominaga. 2020b. tRNA cleavage: a new insight. *Neural regeneration research*. 15:47-52.

Saikia, M., R. Jobava, M. Parisien, A. Putnam, D. Krokowski, X.H. Gao, B.J. Guan, Y. Yuan, E. Jankowsky, Z. Feng, G.F. Hu, M. Pusztai-Carey, M. Gorla, N.B. Sepuri, T. Pan, and M. Hatzoglou. 2014. Angiogenin-cleaved tRNA halves interact with cytochrome c, protecting cells from apoptosis during osmotic stress. *Molecular and cellular biology*. 34:2450-2463.

Saikia, M., D. Krokowski, B.J. Guan, P. Ivanov, M. Parisien, G.F. Hu, P. Anderson, T. Pan, and M. Hatzoglou. 2012. Genome-wide identification and quantitative analysis of cleaved tRNA fragments induced by cellular stress. *J Biol Chem*. 287:42708-42725.

Su, Z., C. Kuscu, A. Malik, E. Shibata, and A. Dutta. 2019. Angiogenin generates specific stress-induced tRNA halves and is not involved in tRF-3-mediated gene silencing. *J Biol Chem*. 294:16930-16941.

Thomas, S.P., T.T. Hoang, V.T. Ressler, and R.T. Raines. 2018. Human angiogenin is a potent cytotoxin in the absence of ribonuclease inhibitor. *Rna*. 24:1018-1027.

Tuorto, F., R. Liebers, T. Musch, M. Schaefer, S. Hofmann, S. Kellner, M. Frye, M. Helm, G. Stoecklin, and F. Lyko. 2012. RNA cytosine methylation by Dnmt2 and NSun2 promotes tRNA stability and protein synthesis. *Nature structural & molecular biology*. 19:900-905.

Yamasaki, S., P. Ivanov, G.F. Hu, and P. Anderson. 2009. Angiogenin cleaves tRNA and promotes stress-induced translational repression. *The Journal of cell biology*. 185:35-42.

Zhou, R., A.S. Yazdi, P. Menu, and J. Tschopp. 2011. A role for mitochondria in NLRP3 inflammasome activation. *Nature*. 469:221-225.

Figure legends:

Figure 1: Analysis of cytosolic (A) and mitochondrial (B) tRNA cleavage after ischemia-reperfusion injury in rats after 24 hours of reperfusion. 4µg total RNA were used per lane (sample). RNA concentration was confirmed immediately prior to electrophoresis. **A:** Cytosolic tRNAs Arg^{CCT} and Met^{CAT} were not cleaved while Gly^{GCC}, Ala^{AGC} and Gln^{CTG} were cleaved canonically (white arrow), although Gln^{CTG} needed extended exposure to show the tiRNA fragments. Leu^{AAG} was robustly cleaved after MCAO, however, we observed a non-canonical fragment (red arrow) to be present in sham animals as well as after MCAO, suggesting a physiologic role. **B:** Mitochondrial tRNAs were cleaved canonically (mt-Gly^{GCC}, mt-Arg^{TCG}; red arrow), non-canonically (mt-Tyr^{GTA}, mt-Ala^{TGC}; red arrow) or show both modes of cleavage (mt-Asn^{GTT}, mt-Met^{CAT}).

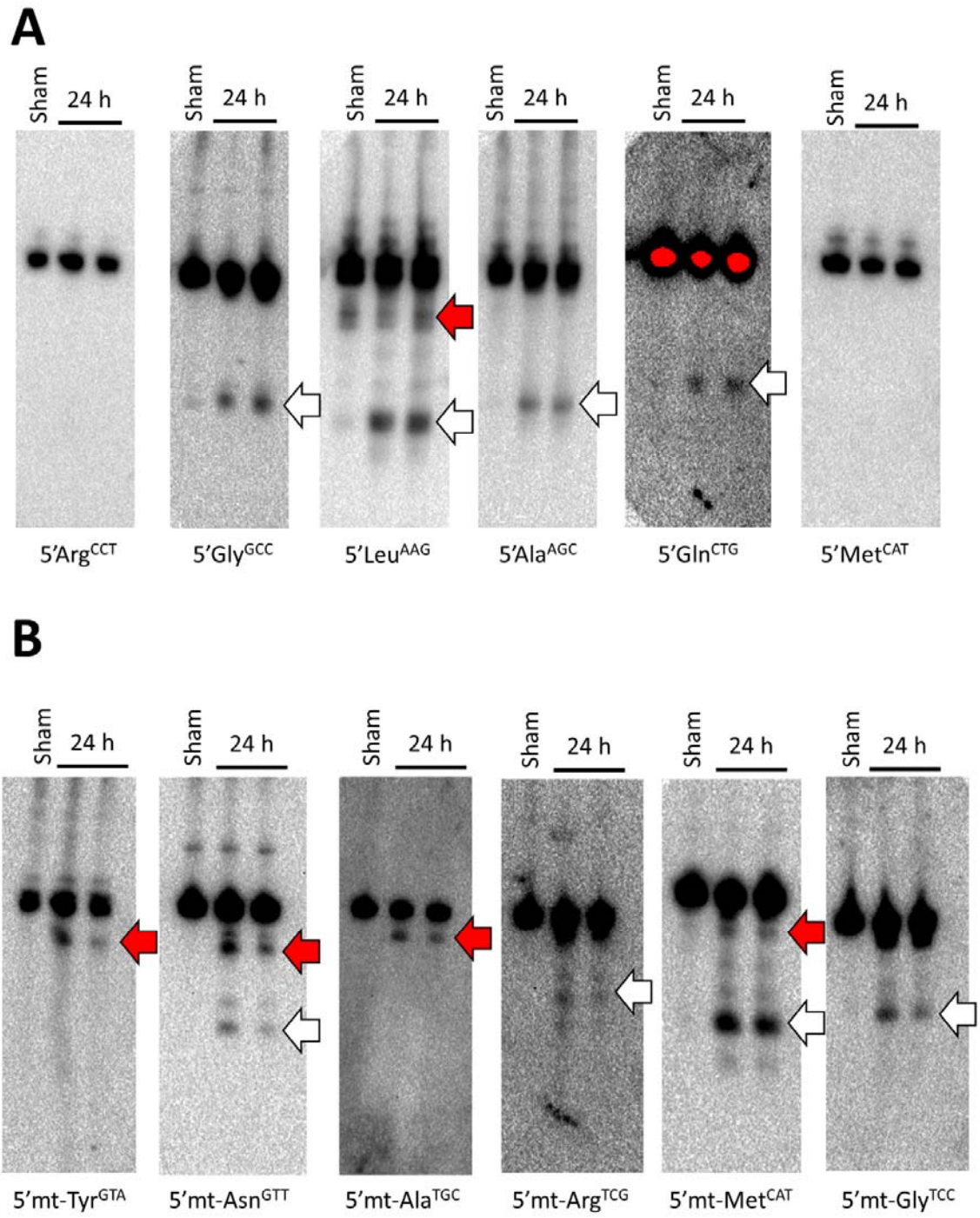
A
Sham
24 h
5'Arg^{CCT}
5'Gly^{GCC}
5'Leu^{AAG}
5'Ala^{AGC}
5'Gln^{CTG}
5'Met^{CAT}
B
5'mt-Tyr^{GTA}
5'mt-Asn^{GTT}
5'mt-Ala^{TGC}
5'mt-Arg^{TCG}
5'mt-Met^{CAT}
5'mt-Gly^{TCC}

Figure 2: Analysis of cytosolic tRNA cleavage in B35 and PC12 cell lines after arsenite (As) or antimycin (A.M) stresses. Cells were exposed to As (1mM) or A.M (200µg/ml) for 4 hours (B35) or 6 hours (PC12). 3µg total RNA were loaded per lane (sample). White arrow: Canonical fragments, red arrow: non-canonical fragments. **A:** Leu^{AAG} was cleaved canonically in B35 after both stresses, while it was cleaved canonically after As and non-canonically after A.M in PC12 cells. **B:** Gly^{GCC} was cleaved canonically after As in PC12 and after As and A.M in B35 cells. Gly^{GCC} needed extended exposure duration to reveal the tiRNA fragments. **C:** Ala^{AGC} was cleaved after As in PC12 cells (also needed extended exposure) while it was minimally canonically cleaved after As in B35 cells and canonically and non-canonically cleaved after A.M stress. **D:** Gln^{CTG} was not cleaved in PC12, while it was cleaved canonically after As and canonically and non-canonically after A.M in B35 cells. **E:** Met^{CAT} was not cleaved in either cell lines. **F:** Arg^{CCT} was only cleaved non-canonically after A.M in B35 cells. **G:** Lys^{CTT} was cleaved into 2 5'tiRNA fragments after As in PC12 cells, both fragments were within the range of the canonical fragments, suggesting that at least one of them was cleaved off the anti-codon (i.e. non-canonical cleavage). But we cannot identify clearly which one at the moment. B35 cells showed the same pattern after As and A.M with an additional non-canonical fragment after A.M (can be better viewed in supplementary figure 2). **H:** Glu^{CTC} was cleaved canonically after As in PC12 and canonically and via both modes after As and A.M in B35 respectively. **Shorter exposure images are provided in supplementary figure 2 for Gly^{GCC} in B35 and PC12, Ala^{AGC} in PC12 and for Lys^{CTT} in B35.**

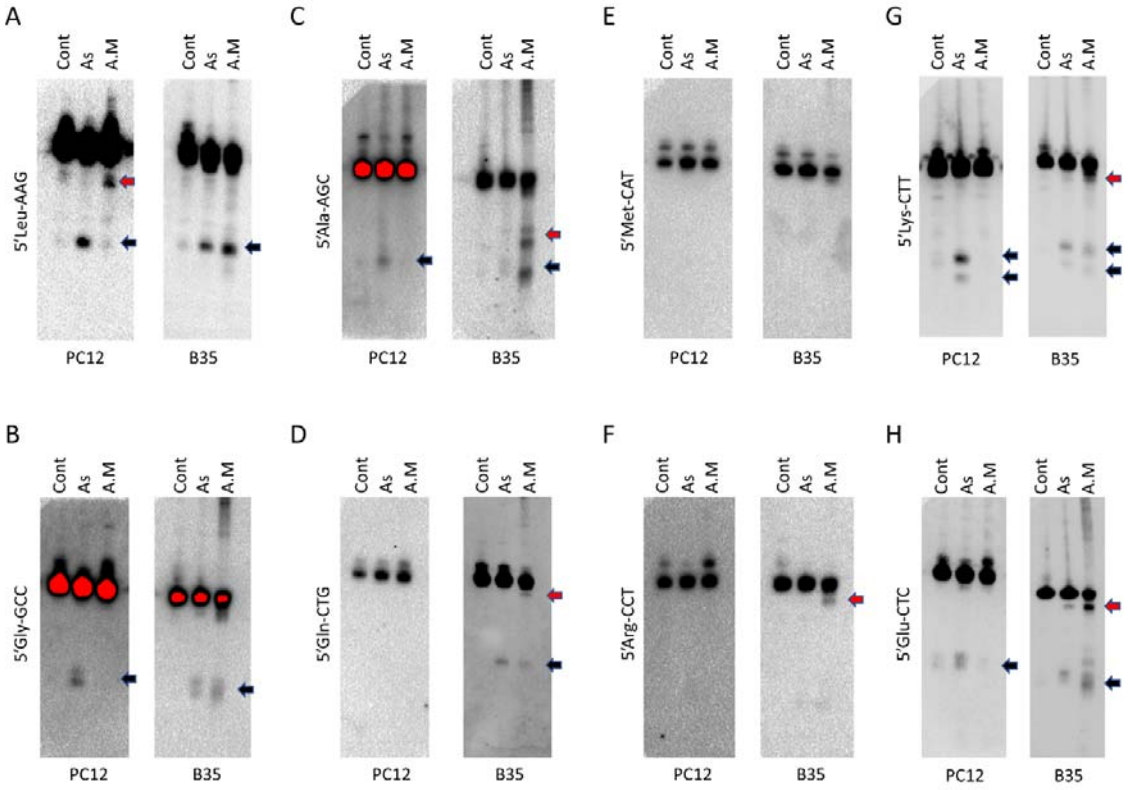
A
5'Leu-AAG
Cont
As
A.M
PC12
B35
B
5'Gly-GCC
C
5'Ala-AGC
D
5'Gln-CTG
E
5'Met-CAT
F
5'Arg-CCT
G
5'Lys-CTT
H
5'Glu-CTC

Figure 3: Analysis of cytosolic tRNA cleavage in B35 and PC12 cell lines after arsenite (As) or antimycin (A.M) stresses. A: mt-Tyr^{GTA} was cleaved Canonically and non-canonically after As stress in PC12 and A.M stress in B35. **B:** mt-Met^{CAT} was cleaved non-canonically after As and A.M stresses in PC12, albeit more robust after As stress. It was not cleaved in B35 cells. mt-Ala^{TGC} (**C),** mt-Asn^{GTT} (**D**), mt-Gly^{TCC} (**E**), and mt-Arg^{TCG} (F) were not cleaved in both cell lines.

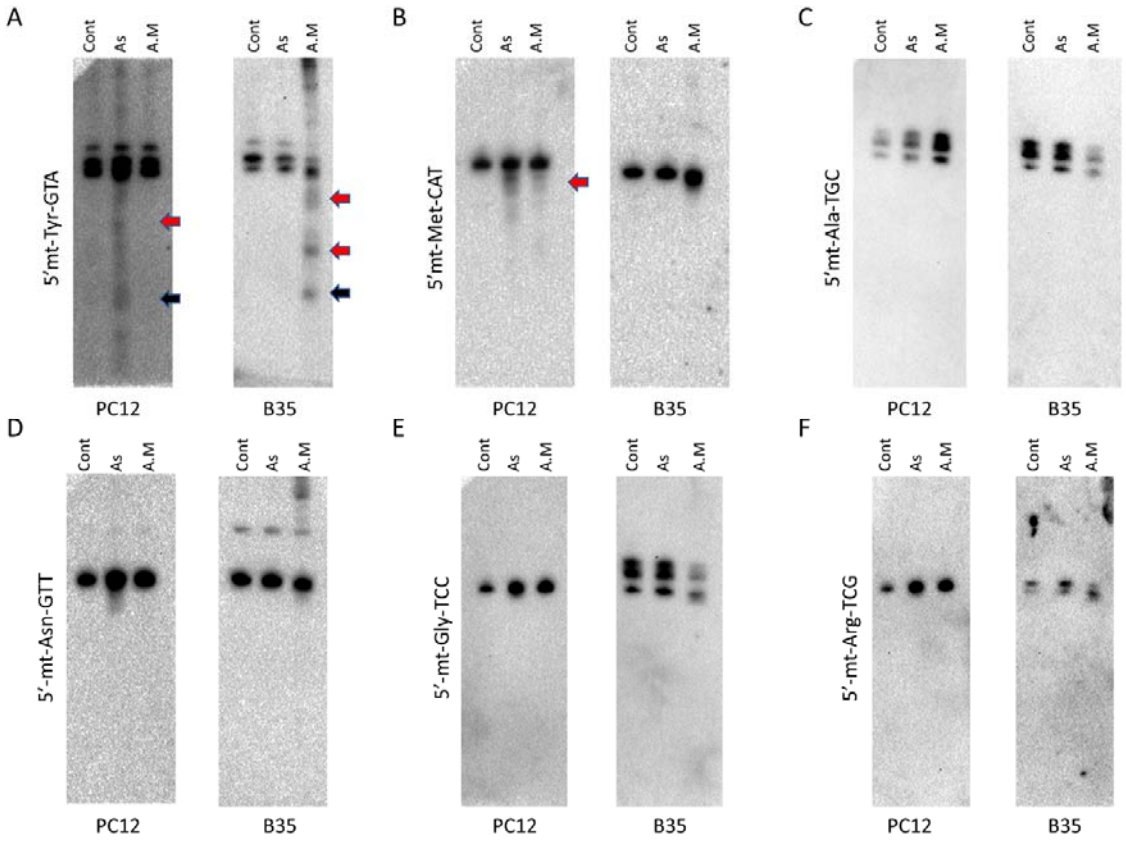

Figure 4: Plasmid hAng or RNH1 overexpression in PC12 and their impact on tRNA cleavage after stress. A: western blotting confirmation of Flag labeled human angiogenin expression in PC12. **B:** Western blotting confirmation of RNH1 overexpression after plasmid induction. RNH1 expression increased 2.5 folds when corrected to beta-actin expression (graph represent relative quantification using ImageJ). **C:** SYBR gold staining after hAng overexpression and stress shows that hAng overexpression increased tRNA cleavage after As stress only and had not impact on A.M stress. **D:** RNH1 overexpression did not suppress tRNA cleavage after As stress. Arrow: tRNA, dotted line: tiRNA.

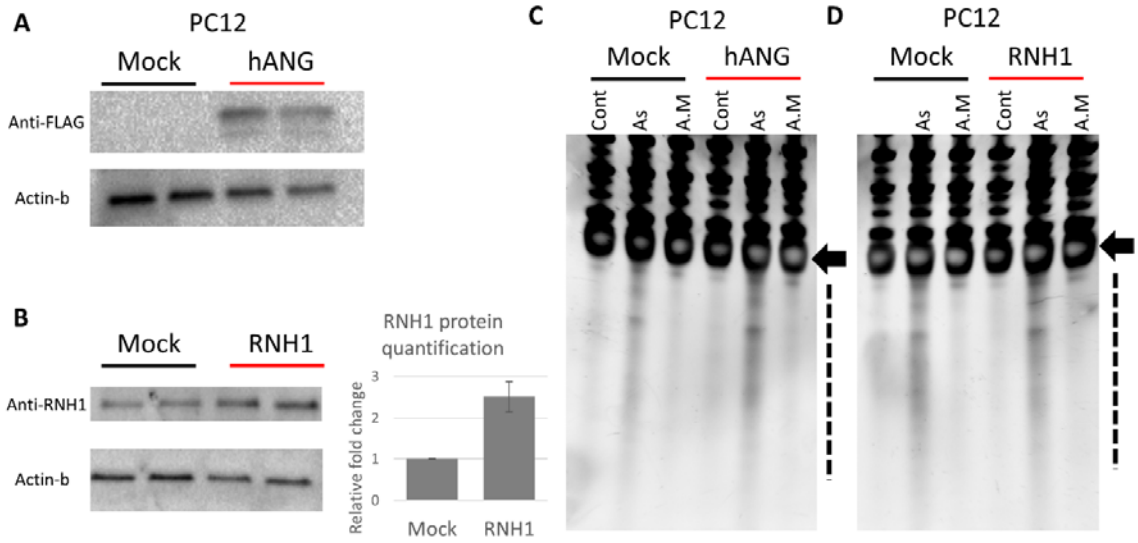
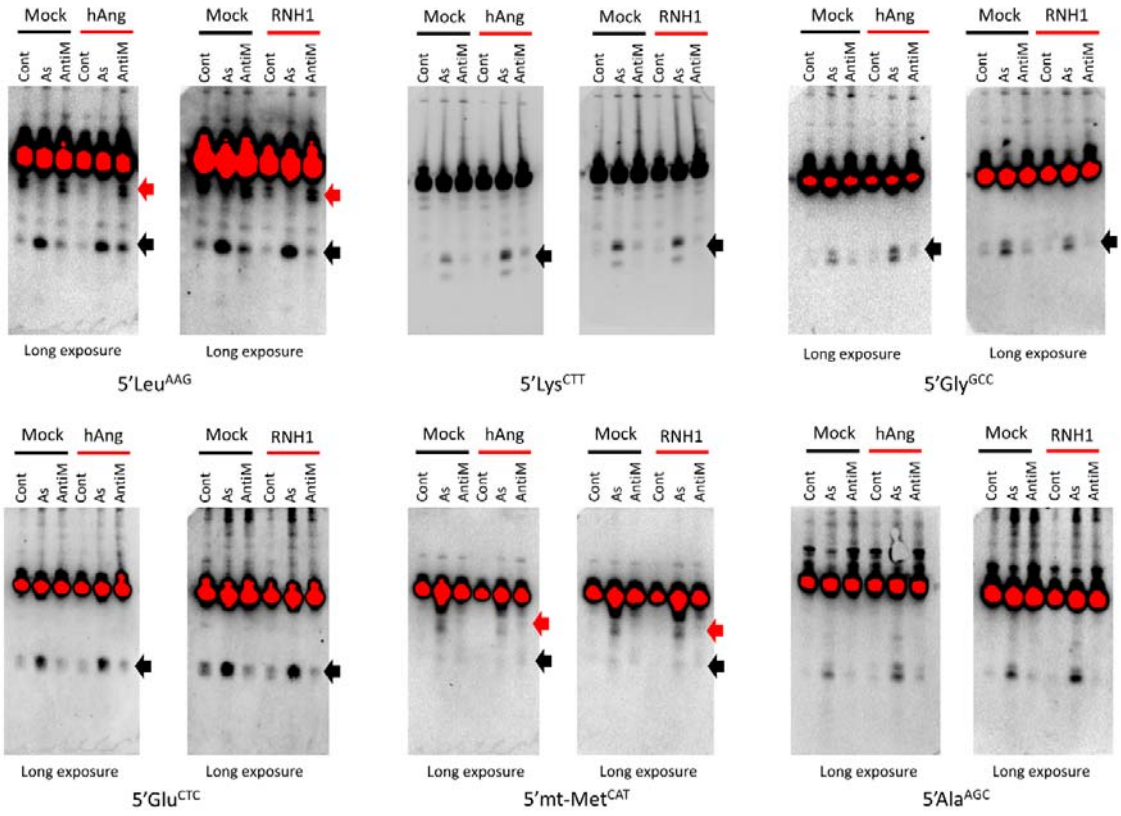
Figure 5: Impact of hANg or RNH1 overexpression on stress induced tRNA cleavage. Specific tRNAs were probed using DIG-labeled probes to evaluate the impact of hANg or its inhibition by RNH1 on their cleavage in PC12 cells. hAng and RNH1 had no effect on the non-canonical fragments in Leu^{AAG} and mt-Met^{CAT}, and even showed a paradoxical response in the latter with RNH1 moderately increasing the non-canonical cleavage. The impact of hANg was stress specific and also tRNA specific, impacting selected tRNAs under either As or A.M or under both stresses depending on the tRNA species. Black arrow: canonical fragments, red arrow: non-canonical fragments. Shorter exposure images for the overexposed blots are presented in supplementary figure 3.